

# Naloxone Ameliorates Retinal Lesions in *Ccl2/Cx3cr1* Double-Deficient Mice via Modulation of Microglia

Defen Shen,<sup>1</sup> Xiaoguang Cao,<sup>1,2</sup> Lian Zhao,<sup>3</sup> Jingsheng Tuo,<sup>1</sup> Wai T. Wong,<sup>3</sup> and Chi-Chao Chan<sup>1</sup>

**PURPOSE.** The role of naloxone, an opioid receptor antagonist, on microglial inhibition and neuroprotective effects has been reported in lipopolysaccharide (LPS)-induced neurodegeneration and light-induced photoreceptor degeneration. The authors evaluated the effects of naloxone on *Ccl2*<sup>-/-</sup>/*Cx3cr1*<sup>-/-</sup> (DKO) mice, a murine model of age-related macular degeneration (AMD).

**METHODS.** Two-month-old DKO and wild-type controls were given daily intraperitoneal injections of naloxone or PBS for 2 months. Animals were examined monthly by funduscopy. Ocular tissue was analyzed histologically and in retinal flat mount preparations. Ocular A2E was measured using HPLC. Quantitative RT-PCR analyzed TNF- $\alpha$ , *IL-1 $\beta$* , *IL-10* and *TLR4* transcripts in the DKO eyes and LPS activated culture microglial cells. Serum nitrite was measured using Griess colorimetric reaction.

**RESULTS.** Naloxone ameliorated the clinical progression and severity of retinal lesions in the DKO mice compared with those of untreated controls. Histopathology also showed less focal retinal degeneration in the treated DKO mice than in controls. The aggregation of microglia in the outer retina in DKO mice was significantly reduced in naloxone-treated animals compared with control untreated DKO. Ocular TNF- $\alpha$ , *IL-1 $\beta$* , and *TLR4* transcripts and A2E were significantly lower in naloxone-treated DKO animals and cultured microglial cells than in controls, as were serum nitrite levels.

**CONCLUSIONS.** Naloxone significantly reduces the progress of retinal lesions in DKO mice. Naloxone modulates microglia accumulation and activation at the site of retinal degeneration, which may be mediated by inhibition of the proinflammatory molecules of NO, TNF- $\alpha$ , and IL- $\beta$ . The potential therapeutic effects of naloxone on retinal degeneration, including AMD, warrants further investigation. (*Invest Ophthalmol Vis Sci*. 2011;52:2897-2904) DOI:10.1167/iov.10-6114

Naloxone is a synthetic and nonselective antagonist of G-protein-linked classic opioid receptors widely expressed in the central and peripheral nervous systems. This drug is used

in the standard treatment of heroin overdose. Structurally, naloxone closely resembles the naturally occurring opiate morphine and binds to opioid receptors in a stereospecific manner with L-naloxone as the functional enantiomer.<sup>1,2</sup> The neuroprotective effect of naloxone has been demonstrated in an in vitro neuron/glia culture system<sup>3,4</sup> and in in vivo lipopolysaccharide (LPS)-induced neurodegeneration and Parkinson's disease models.<sup>5,6</sup> These effects are unlikely to be related to the opioid system because both L- and D-isomers of naloxone can effectively inhibit microglial activation and the production of NO, TNF- $\alpha$ , and superoxide-free radicals.<sup>7-9</sup>

Microglia in the brain and retina have a myeloid origin and enter the CNS during embryological development and serve to maintain normal retinal function in the adult animal.<sup>10</sup> They are activated by retinal injury and degeneration, transforming from a stellate, ramified morphology to an amoeboid shape. These activated microglia proliferate, migrate to areas of injury, phagocytize debris, secrete proinflammatory cytokines and chemokines, and can also exert neurotoxic effects.<sup>11</sup> In the young healthy retina, microglia are located in the inner retina<sup>12</sup>; however, with aging, they can migrate to the outer retina and the subretinal space.<sup>13</sup> Activated microglia have also been reported to accumulate in the lesions of various neurodegenerative diseases, including age-related macular degeneration (AMD). The accumulation and activation of microglia may constitute the important aspects of chronic neuroinflammation that trigger neurodegeneration.<sup>14-17</sup> Inhibition of microglial activation has been found to promote neuronal survival and to protect against neurodegenerative changes.<sup>7,18,19</sup>

Recently, the neuroprotective effect of naloxone in a rat model of light-induced photoreceptor degeneration has been reported through the inhibition of activated microglia.<sup>20</sup> However, there are controversial data regarding the effect of naloxone on neuronal damage and its role on activated microglia: naloxone is reported to inhibit the protection against LPS plus IFN- $\gamma$ -induced microglial injury under morphine,<sup>21</sup> but naloxone is also reported to effectively block microglial involvement in the combined Mn and LPS neurotoxicity.<sup>22</sup> *Ccl2*<sup>-/-</sup>/*Cx3cr1*<sup>-/-</sup> (DKO) mice develop focal retinal lesions that progress with age and resemble macular lesions found in AMD in both clinicopathologic and biochemical aspects.<sup>23,24</sup> Microglial activation and accumulation are also commonly observed in the retinas of DKO mice.<sup>25</sup> In this study we evaluated the effect of naloxone on the activated microglia in the retinal AMD-like lesions of DKO mice.

## MATERIALS AND METHODS

This study was conducted in compliance with the ARVO Statement for the Use of Animals in Ophthalmic and Vision Research. All animal experiments were performed under the protocols approved by the National Eye Institute Institutional Animal Care and Use Committee.

From the <sup>1</sup>Immunopathology Section, Laboratory of Immunology, and the <sup>3</sup>Unit of Neuronal and Glial Interactions in Retinal Disease, National Eye Institute, National Institutes of Health, Bethesda, Maryland; and the <sup>2</sup>Department of Ophthalmology, People's Hospital, Peking University, Beijing, China.

Supported by the National Eye Institute Intramural Research Program.

Submitted for publication June 24, 2010; revised October 4 and November 10, 2010; accepted November 10, 2010.

Disclosure: D. Shen, None; X. Cao, None; L. Zhao, None; J. Tuo, None; W.T. Wong, None; C.-C. Chan, None

Corresponding author: Chi-Chao Chan, Building 10, Room 10N103, 10 Center Drive, NIH/NEI, Bethesda, MD 20892-1857; chanc@nei.nih.gov.

## Animals

The development of DKO mice has been described previously.<sup>23</sup> DKO mice demonstrate a broad spectrum of AMD-like pathologic features that have early onset and high penetrance. These features include focal retinal lesions visible on funduscopy and histology. The lesions are characterized by focal RPE, photoreceptor, and outer retinal layer degeneration. In addition, DKO mice exhibit increased ocular A2E accumulation on biochemical analysis and altered innate and adaptive immunities including abnormal patterns of microglial accumulation and migration.<sup>23-25</sup> Wild-type (WT) mice were of the C57BL/6 background. Two independent experiments involving 21 DKO and 20 WT mice were performed.

## Experimental Protocol

Two-month-old DKO and WT mice were given daily intraperitoneal injections of D-naloxone (Sigma, St. Louis, MO) (0.13 mg in 0.1 mL PBS) for a period of 2 months. Control animals of both strains were given 0.1 mL PBS alone on a similar schedule. In the first experiment, 11 mice (6 DKO, 5 WT) received naloxone, and 6 mice (3 DKO, 3 WT) received PBS. In the second experiment, 16 mice (8 DKO, 8 WT) received naloxone, and 8 mice (4 DKO, 4 WT) received PBS. Funduscopy examinations were conducted at monthly intervals. Experimental animals were euthanized 2 months after treatment, and sera and eyes were collected for analyses.

## Funduscopy Photography

Experimental animals were administered systemic anesthesia before fundus photography. Tropicamide ophthalmic solution (1%) (Alcon Inc., Fort Worth, TX) was used for pupillary dilation. After pupillary dilation, an endoscope (Karl Storz, El Segundo, CA) coupled with a digital camera was used for fundus photography, which was documented as the presence of deep focal retinal lesions, pigmentary alterations, retinal vascular, and optic nerve head abnormalities. Fundus photographs were captured in the same area over repeated examinations and graded by a masked observer. Sequential photographs were scored for the presence of progression or regression according to a previous publication.<sup>26</sup> Progression was defined as a >10% increase of deep retinal and subretinal spot (lesion) number, >50% increase in spot diameter in at least one-third of the spots, >5 fused spots, or >2 chorioretinal scars in comparison with the previous observation. Regression was defined as a >10% decrease of deep retinal lesion number and a >50% decrease in spot diameter in at least one-third the spots.

## Histopathology

Harvested eyes were fixed in 10% formalin for at least 24 hours and then embedded in methacrylate. In the first experiment, 8 eyes from 4 DKO and 4 WT mice that were treated with naloxone and 6 eyes from 3 DKO and 3 WT that received PBS were collected for histopathology. In the second experiment, 16 eyes from 16 mice (4 eyes from 4 mice in each group) were collected for histopathology. The eyes were serially sectioned through the vertical pupillary-optic nerve plane. Six initial sections were cut and stained with hematoxylin and eosin. If an ocular lesion (e.g., photoreceptor degeneration, dystrophy, atrophy, RPE abnormalities, chorioretinal neovascularization) was observed in the initial sections (4  $\mu\text{m}$  thick), another 6 to 12 sections would be cut through the lesion. These slides were also stained with periodic acid Schiff to highlight the Bruch's membrane and the basement membrane of small neovascular vessels. The severity of retinal lesions was compared with the mean percentage of the whole retina that contained degenerative lesions in each group.

## Immunohistochemistry in Retinal Flat Mounts

Immunohistochemistry in retinal flat mounts was conducted as previously described.<sup>27</sup> Briefly, retinal tissue was gently dissected free from other ocular structures as an intact sheet and fixed in 4% paraformaldehyde in 1 $\times$  PBS (pH 7.3), and retinal flat mounts with the photore-

ceptor layer positioned uppermost were prepared. Immunohistochemical staining was performed on the sections with Alexa 555-conjugated peanut agglutinin (PNA) to label cone outer-segment sheaths to mark the position of the outer retina. Staining with 4',6-diamidino-2-phenylindole (DAPI; 1:1000), a nuclear marker, was also used. Immunohistochemical staining with primary antibodies to ionized calcium-binding adaptor molecule-1 (Iba1; Wako Chemicals, Richmond, VA), a marker constitutively expressed by microglia, and major histocompatibility complex (MHC) class II, a marker often expressed on activated microglia, were also performed. The stained retinal tissue was examined and counted for microglia under a confocal microscope (SP2; Leica, Bannockburn, IL).

## A2E Extraction and Quantification

2-[2,6-Dimethyl-8-(2,6,6-trimethyl-1-cyclohexen-1-yl)-1E,3E,5E,7E-octatetra-enyl]-1-(2-hydroxyethyl)-4-[4-methyl-6(2,6,6-trimethyl-1-cyclohexen-1-yl) 1E,3E,5E,7E-hexatrienyl]-pyridinium (A2E) is the major component of lipofuscin fluorophores generated from the visual cycle flux of all-trans-retinal. The molecule is particularly relevant to aging and AMD pathogenesis.<sup>28</sup> The mice were kept in the dark for >12 hours before being killed. A2E in the eye was extracted with chloroform/methanol, as previously described.<sup>26</sup> Detection and quantification was performed (1100 LC system; Agilent, Wilmington, DE). A gradient of 50% to 90% acetonitrile (T. J. Baker, Phillipsburg, NJ) in 0.1% trifluoroacetic acid (T. J. Baker) was used to separate A2E on a C18 column (Zorbax; Agilent) at a flow rate of 1 mL/min. A2E was quantified using external A2E standards.

## RNA Isolation and Quantitative Real-Time PCR

Total RNA was isolated from mouse eyes by an extraction method (TRIzol-phenol-chloroform; Invitrogen, Carlsbad, CA). RNA yield and purity were determined photometrically with a spectrophotometer (DU640; Beckman Coulter, Fullerton, CA). Real-time polymerase chain reaction (PCR) enables quantitative detection of small amounts of mRNA. After the usual isolation of RNA, the total RNA was transferred to complementary DNA (cDNA) using reverse transcriptase (SuperScript II; Invitrogen). cDNA was then used for the specific PCR. Relative quantification of gene expression was performed with specific primers using a quantitative (q) PCR system (MX3000P; Agilent, La Jolla, CA) and qPCR primer assays kits (SA Biosciences, Frederick, MD). All primers and probes were designed to cross intron/exon boundaries to avoid amplification of genomic DNA. Each 25- $\mu\text{L}$  reaction volume contained 1 $\times$  PCR master mix (SYBR Green/Rox; SA Biosciences, Frederick, MD), 0.4  $\mu\text{M}$  of each primer, and 2  $\mu\text{L}$  cDNA.

The cDNA was amplified with specific primers for 40 cycles.  *$\beta$ -Actin* (primers 5'-CCCAGCACAAATGAAGATCAA-3' and 5'-ACATCTGCTGGAAGTGGAC-3') was simultaneously processed in the same sample as an internal control. The levels of *TNF- $\alpha$* , *IL-1 $\beta$* , *IL-10*, and *TLR4* gene expression primed by RT<sup>2</sup> qPCR primers (SA Biosciences) were determined as the relative ratio to compare with the same gene expression in a universal RNA. The relative expression in gene change was calculated by comparative  $\Delta\Delta\text{CT}$  methods. All experiments were performed at least twice.

## Mouse Retinal Microglia Cells: In Vitro Experiment

Culture of mouse retinal microglia cells was obtained as previously described.<sup>29</sup> Briefly, microglia were isolated from retinas of young C57BL/6 mice (postnatal day [P] 10-P30). Isolated retinas separated from RPE cells were cultured. After the mixed culture had grown confluent, microglia were found distributed on the top of the cell layer and could be detached by shaking the flask by hand. These retinal microglia were incubated overnight with various dosages of LPS exposure. After LPS exposure, the microglia were divided into two groups: those with and those without naloxone (1  $\mu\text{M}$ ) for 24 hours. The cells were then harvested. Total RNA was isolated and subjected to qPCR, as described.

### Measurement of Serum Nitrite

Serum nitrite levels were measured using the colorimetric Griess assay.<sup>30</sup> Briefly, 20  $\mu$ L serum was diluted with distilled water to 500  $\mu$ L and mixed with equal volume Griess reagent, containing 1.0% sulfanilamide, 0.1% *N*-(1-naphthyl) ethylenediamine dihydrochloride, and 2.5% phosphoric acid (Sigma-Aldrich, St. Louis, MO). Absorbency was read at room temperature by a spectrophotometer (DU640; Beckman Coulter) at 550 nm in reference to a standard nitrite quantitative curve.

### Statistical Analysis

Statistical analyses were compared by  $\chi^2$  test. Multiple means were compared by one-way analysis of variance, followed by Duncan's multiple-range test for post hoc comparison of means. Differences were considered significant when  $P < 0.05$ .

## RESULTS

The two independent repeated experiments yielded reproducible results. Experimental end-point data (funduscopy, histopathology, immunohistochemistry, and A2E) were pooled and presented as described.

### Naloxone Slowed the Progression of DKO Retinal Lesions

Mean funduscopy examination scores from baseline to 2 months increased in control DKO mice ( $+1.36 \pm 0.32$  points) but decreased in treated DKO mice ( $-0.75 \pm 0.28$  points). The effect of naloxone treatment in DKO mice was discernible after only 1 month of treatment. The treated DKO mice demonstrated slower progression than the PBS-injected control DKO mice ( $-0.32 \pm 0.25$  vs.  $+1.21 \pm 0.29$ ;  $P = 0.001$ ). Representative funduscopy photographs were illustrated in Figure 1.

Naloxone administration to WT mice for 2 months had no effect on retinal structure.

The clinical effect of naloxone was confirmed by ocular histology and biochemistry. Histopathologic studies found that the mean percentage of the retinal area that contained degenerative lesions in control DKO mice ( $38.70\% \pm 9.80\%$ ) was higher than in the naloxone-treated DKO mice ( $18.00\% \pm 13.10\%$ ) ( $P = 0.048$ ). Naloxone-treated mice also had smaller focal retinal lesions and less extensive loss of photoreceptors (Fig. 2). The frequency of focal retinal abnormalities such as photoreceptor and RPE degeneration was lower in the treated mice than in the untreated controls. Ocular A2E measured significantly lower in naloxone-treated DKO mice ( $12.92 \pm 4.35$  pM) than in control DKO mice ( $18.19 \pm 2.06$  pM) ( $P = 0.016$ ).

### Naloxone Decreased Ocular Expression of Proinflammatory Cytokines, TLR4, and Serum Nitrite but Leveled Ocular Expression of IL-10 in DKO Mice

Naloxone-treated eyes, compared with the eyes of the control WT mice, showed significantly reduced levels of transcripts for the inflammatory related molecules *TNF- $\alpha$*  ( $P < 0.001$ ), *IL-1 $\beta$*  ( $P = 0.049$ ), and *IL-10* ( $P = 0.036$ ) but not for *TLR4* ( $P = 0.700$ ). Similarly, *TNF- $\alpha$* , *IL-1 $\beta$* , and *TLR4* expression levels were significantly reduced ( $P = 0.006$ ,  $P = 0.004$ , and  $P = 0.014$ , respectively) in DKO mice after naloxone treatment (Figs. 3A-D). However, *IL-10* mRNA levels in DKO mice did not change significantly ( $P = 0.119$ ). The results are illustrated in Figure 3.

Serum nitrite concentrations were  $8.27 \pm 3.20$   $\mu$ M in untreated WT,  $5.74 \pm 0.20$  in naloxone-treated WT ( $P > 0.05$ ),  $10.64 \pm 3.17$  in untreated DKO, and  $6.36 \pm 0.92$  in treated DKO

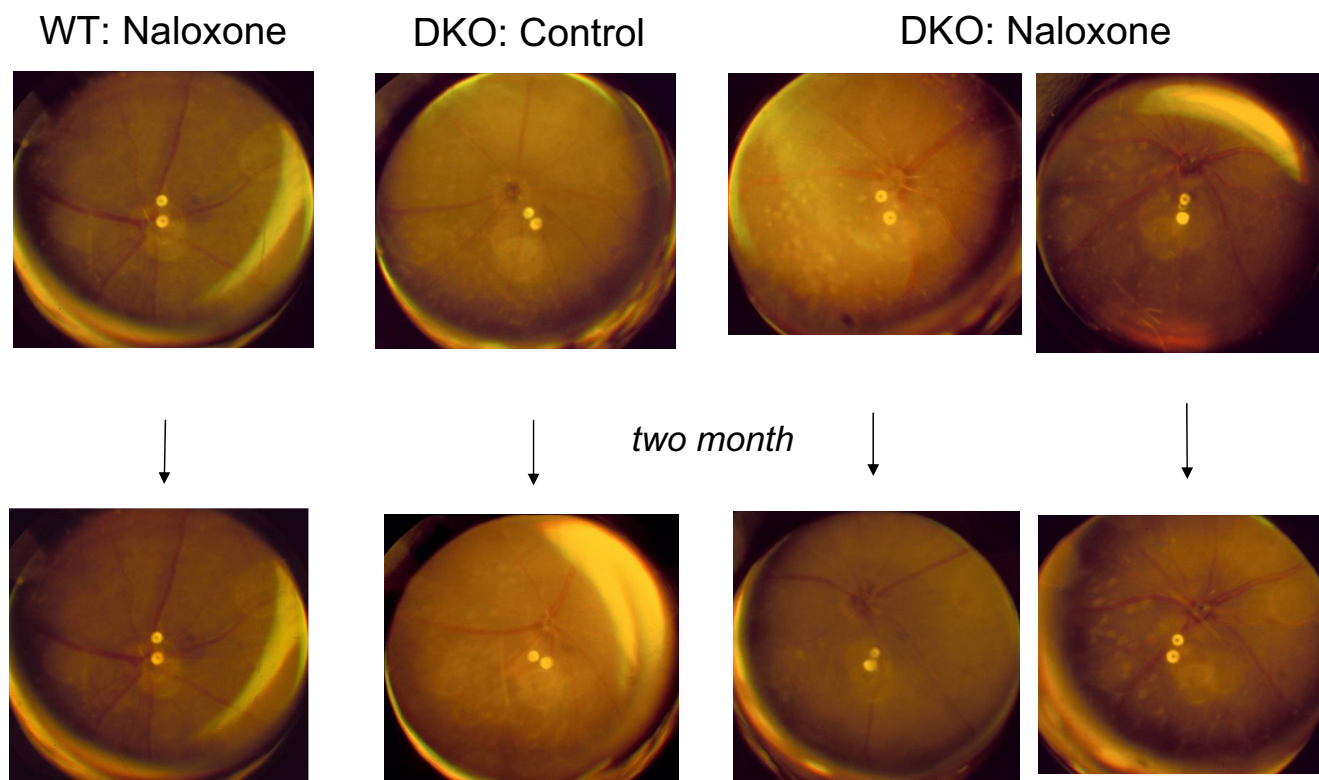


**FIGURE 1.** Fundus photographs at baseline and 2 months after injection. Normal retinas were observed in WT mice that received either PBS or naloxone (column 1). Progressively deep retinal lesions had developed in 2-month-old control DKO mice (column 2), but a slower progression of the lesions were seen in DKO mice treated with naloxone (columns 3, 4).

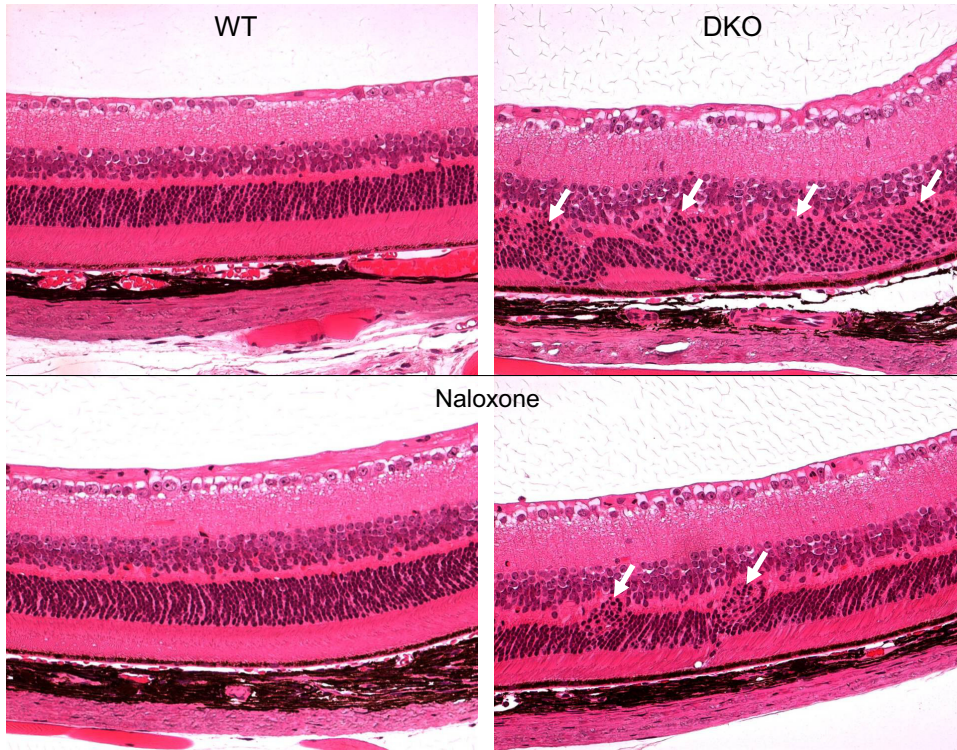


**FIGURE 2.** Photomicrographs of mouse retina. Normal retinal structure was illustrated in both control and naloxone-treated WT mice (*left*). Large foci with photoreceptor degeneration (*arrows*) were noted in DKO control mice (*top, right*), but only small focal photoreceptor disorganization (*arrows*) was found in naloxone-treated DKO mice (*bottom, right*).

mice ( $P = 0.049$ ), respectively. No statistical difference was found in serum nitrite levels between untreated WT and untreated DKO.

**Naloxone Decreases Retinal Microglia Accumulation and Activation in the Outer Retina in *Ccl2*<sup>-/-</sup>/*Cx3cr1*<sup>-/-</sup> Mice**

The effect of naloxone treatment on microglial accumulation in the outer retina was also analyzed in retinal flat mounts

(mounted photoreceptor-side uppermost) in treated and control WT and DKO mice. Few Iba1-positive microglia were detected in the outer retina in both treated and control WT animals; however, in control DKO animals, large numbers of strongly Iba1-positive microglia were found in the outer retina at the level of the photoreceptors. By comparison, in naloxone-treated DKO mice, microglia in the outer retina were fewer in number, stained less intensely for Iba-1, and had a more rami-

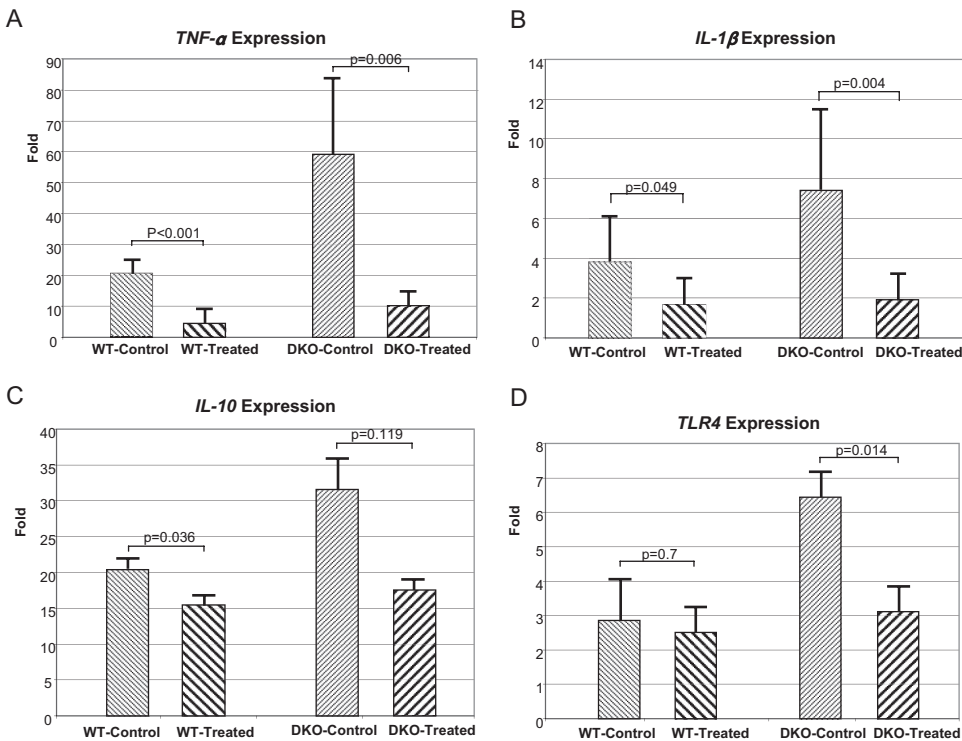
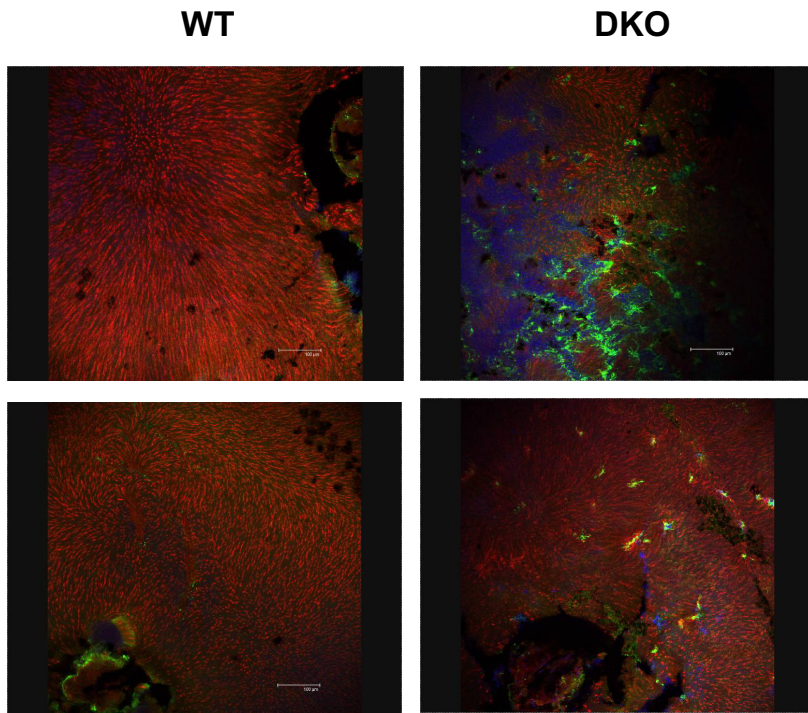


**FIGURE 3.** Transcript expression of ocular *TNF-α*, *IL-1*, *IL-10*, and *TLR4*. The transcript levels in the eyes were higher in DKO control than in WT control mice. Naloxone treatment reduced the expression level in both strains of mice. The reported fold changes in mRNA levels using the  $\Delta\Delta CT$  method were reported relative to the calibrator, the universal gene expression, which has a value of 1.

**FIGURE 4.** Microglial distribution in control and naloxone-treated WT and DKO mice in the outer retina. Microglial accumulation in the outer retina was visualized in retinal flat mounts (mounted with photoreceptor-side uppermost) by immunohistochemical staining with Iba1 (green). Outer retinal cone sheaths were labeled with Alexa-555 conjugated PNA (red), marking their position in the outer retina. In WT retinas, few microglia were observed in the outer retina in both treated and control animals (left). In DKO retinas, clusters of aggregated microglia were found in the outer retina in control-treated animals (top, right), but comparatively fewer microglia were observed in the naloxone-treated animals (bottom, right).

Control  
No treated

Naloxone  
Treated



fied morphology than control DKO animals, suggestive of a less activated phenotype (Fig. 4). Quantification of microglia in the outer retina revealed that treated DKO animals had significantly reduced microglial numbers, both within the central retina and within retinal lesions, compared with control DKO animals (Fig. 5). Differences in outer retinal microglial numbers between control and treated WT animals, because of the small number of microglia found, were not statistically significant ( $P = 0.45$ ).

**Naloxone Suppressed LPS-Induced Proinflammatory Molecular Expression In Vitro**

Without LPS, retinal microglia (Fig. 6) produced few IL-1 $\beta$  (1.4-fold), IL-10 (1.2-fold), TLR-4 (1.4-fold), and TNF- $\alpha$  (1.4-

fold) transcripts in normal culture medium (Fig. 7). LPS exposure significantly increased these proinflammatory molecules in a dose-response relationship (TNF- $\alpha$ , 6- to 9-fold; IL-1 $\beta$ , 2- to 5-fold; TLR-4, 3- to 6-fold; and IL-10, 2- to 4-fold). Naloxone treatment considerably lowered the releasing of these molecules, particularly TNF- $\alpha$  expression. When exposure to the highest dosage of LPS (100 ng) or in the most activated state, naloxone significantly decreased the expression of these inflammatory genes on the culture microglia cells.

**DISCUSSION**

In the present study, naloxone significantly reduced the progression of retinal lesions in DKO mice as visualized clinically and on histopathologic examination. Furthermore, retinal A2E levels in the DKO mice treated with naloxone were significantly lower than in the control nontreated DKO mice. Naloxone also decreased microglia accumulation and activation at the site of retinal degeneration, which might possibly have been mediated, at least in part, by the downregulation of inflammatory molecules NO, TNF- $\alpha$ , and IL-1 $\beta$ , that were observed with treatment (Table 1). The downregulation of these proinflammatory molecules is also demonstrated in the activated microglia in vitro, which is in line with recent studies on primary rat mesencephalon microglia.<sup>22</sup> Naloxone is a nonselective antagonist of opioid receptors. It is a  $\mu$ -opioid receptor competitive antagonist; the  $\mu$ 3 receptor is linked to NO production and inflammation mechanism. Acting on these receptors, naloxone may well protect NO-induced neuronal damage.<sup>31,32</sup> Retinal changes in DKO mice are indicative of a chronic, low-grade, neuroinflammatory process.<sup>25</sup> Chronic neuroinflammation involves not only the activation of microglia and the consequent sustained release of various inflammatory mediators but also oxidative and nitrosative stress.<sup>33</sup> Microglial activation can play important roles in controlling or adapting to stress, or both. The activated microglia can adopt different phenotypes, depending on the local diseased tissue environment and on systemic influences. In earlier stages of disease, microglia have the potential to be relatively benign, to contribute to disease progression, or perhaps even to be pro-

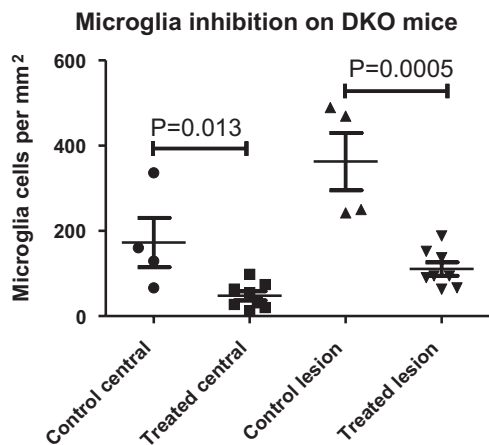


**FIGURE 5.** Microglial accumulation in the outer retina in naloxone-treated and PBS-treated control DKO mice. Overall, microglial densities in the outer retina were quantitated in the central retina within 500  $\mu$ m of the optic nerve (left) in naloxone-treated and control DKO mice. Microglial densities within lesioned areas, which contained the largest accumulations of microglia, were also calculated (right). In both computations, outer retinal microglial density was significantly reduced in treated versus control DKO animals.

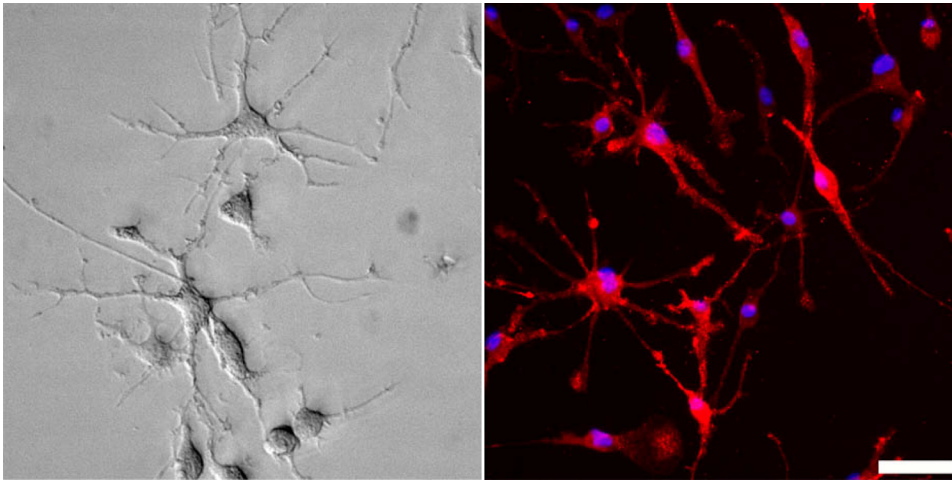


**FIGURE 6.** Retinal microglia in culture. The cultured microglia have many spindly processes emanating from the central cell body. *Left:* bright-field image of cultured retinal microglial cells showing ramified morphology. *Right:* epifluorescence image of culture retinal microglia immunolabeled for Iba-1 (red) and DAPI (blue). All cells in the culture were Iba-1 immunopositive. Scale bar, 25  $\mu$ m.

tective.<sup>34,35</sup> Transplantation of bone marrow-derived stem cells to *rd1* mice was effective in rescuing retinal degeneration, possibly because of the recruitment of bone marrow-derived microglia that are protective of inherited retinal neurovascular degeneration.<sup>36</sup> However, chronic activation of microglia may lead to exaggerated microglial responses, leading to retinal damage and neuronal apoptosis,<sup>11</sup> which have been demonstrated in models of light-induced retinal degeneration,<sup>37,38</sup> animal models of glaucoma,<sup>39,40</sup> and genetic models of various retinal degenerations.<sup>41,42</sup> The slow degeneration of neurons and their processes might also activate microglia. In fact, a positive feedback loop has been hypothesized in which microglia activated by neuronal degeneration secrete neurotoxic molecules, which in turn promote further neurodegeneration, thereby initiating a self-perpetuating degenerative process. Therefore, the accumulation and recruitment of activated microglia in the retinal lesions and subretinal space of the DKO mice can be easily observed.<sup>25</sup>

Microglia with predominantly activated phenotypes have been documented in many chronic neurodegenerative diseases, such as Alzheimer disease,<sup>43</sup> Parkinson disease,<sup>44</sup> and AMD.<sup>17,45,46</sup> In this study, the number of microglia in the DKO treated with naloxone was significantly decreased ( $P = 0.0005$ ). In addition, the treated microglia recovered to normal morphology. Activated microglia often release abundant IL-1 $\beta$  and TNF- $\alpha$ , the two well-studied molecules that promote neuronal degeneration.<sup>47</sup> TNF- $\alpha$  is an inflammatory cytokine and has been found in a subset of microglia that is closely associated with retinal vessels.<sup>48</sup> Anti-TNF- $\alpha$  therapy has been reported to reduce both the size and the leakage of laser-induced choroidal neovascularity in mice.<sup>49</sup> We have also reported higher ocular TNF- $\alpha$  transcripts in the DKO mice that became lower when the retinal lesions were rescued with an omega-3-rich diet in these mice.<sup>26</sup> Similar to TNF- $\alpha$ , IL-1 $\beta$  is produced during neurodegenerative diseases. In a recent study, IL-1 $\beta$  is found to play a crucial role in the activation of microglia by

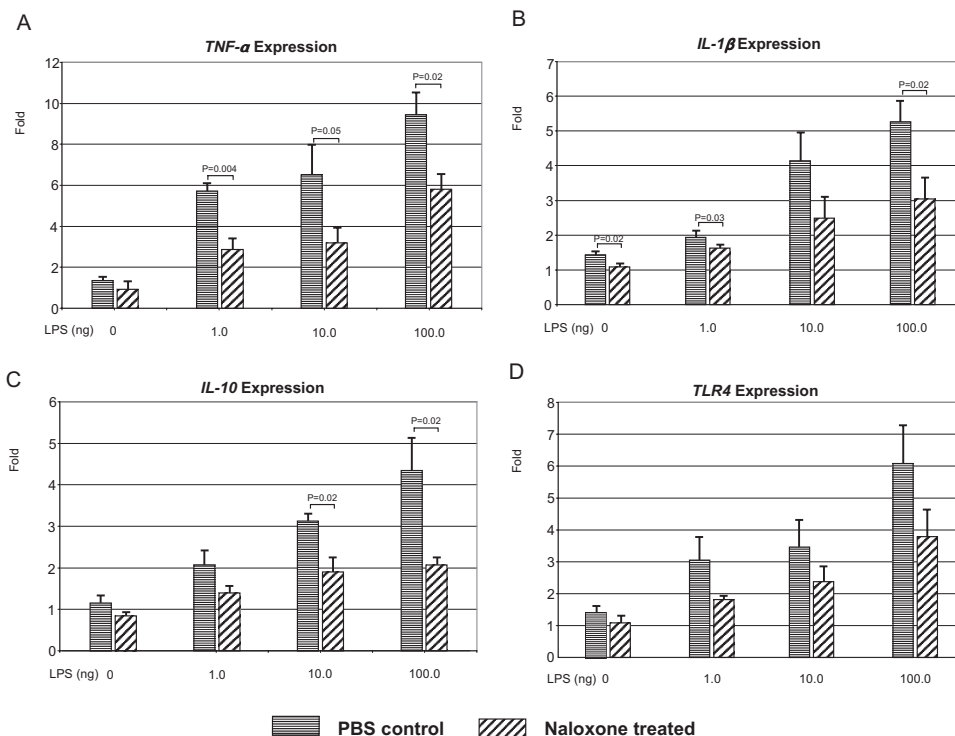


**FIGURE 7.** Transcript expression of culture retinal microglial TNF- $\alpha$ , IL-1, IL-10, and TLR4. LPS induced the release of four inflammatory genes in microglia. Naloxone efficiently blocked the production of inflammatory factors and protected microglia from LPS-induced damage in a dose-dependent response. Results are mean  $\pm$  SEM. The experiment was performed in triplicate.

**TABLE 1.** Expression of Proinflammatory Cytokines and TLR4 Transcripts in Mouse Eye after Naloxone Treatment

	WT Group			DKO Group		
	Control	Treated	P	Control	Treated	P
<i>TNF-α</i>	20.61 ± 2.05	4.57 ± 1.89	<0.001	59.13 ± 10.82	10.28 ± 1.70	0.006
<i>IL-1β</i>	3.81 ± 1.02	1.68 ± 0.57	0.049	7.41 ± 1.83	1.81 ± 0.50	0.004
<i>IL-10</i>	20.43 ± 1.22	15.46 ± 0.79	0.036	31.55 ± 3.09	17.57 ± 0.82	0.119
<i>TLR4</i>	2.86 ± 0.86	2.50 ± 0.44	0.7	6.44 ± 0.45	3.12 ± 0.42	0.014

All values are mean ± SE.

kainic-acid (a neurotoxicant), which results in increased excitability of rat hippocampal neurons in vitro and in vivo.<sup>50</sup> Our present study reveals significant decreases of *IL-1β* and *TNF-α* transcript levels in the naloxone-treated DKO mice, resulting in the suppression of activated microglia and the amelioration of retinal AMD-like lesions.

IL-10 is a potent anti-inflammatory cytokine produced by Th2 lymphocytes, B-lymphocytes, and macrophages. IL-10 suppresses the production of *TNF-α* and *IL-1β*.<sup>51</sup> In a recent study, ultralow-dose naloxone was able to upregulate IL-10 expression and to suppress neuroinflammation in morphine-tolerant rats.<sup>52</sup> However, ocular *IL-10* levels did not change statistically in the naloxone-treated DKO mice compared with the control mice.

Toll-like receptor (TLR)-4, 1 of 10 mammalian paralogs with homology to the *Drosophila* protein Toll, is the central component of the LPS receptor.<sup>53</sup> The highly specific LPS-sensing function of TLR4 is known to display exquisite sensitivity to LPS. Exposure of microglia to LPS results in the initiation of intracellular cascades, leading to the nuclear translocation of NF-κB and the expression of proinflammatory mediators including NO and *TNF-α*. This process depends on the binding of LPS to microglial cellular surface membrane receptors TLR4 and CD14.<sup>54</sup> In the CNS, TLR4 is expressed predominantly by microglia when activated by various endogenous or exogenous molecules, lead to microglia activation, and release proinflammatory cytokines including *TNF-α* and *IL-1β*.<sup>55</sup> Recently, naloxone was reported to attenuate MnCl<sub>2</sub> and LPS-induced free radical generation (NO), cytokine release (*TNF-α* and *IL-1β*), and dopaminergic neurotoxicity through the involvement of microglia.<sup>22</sup> Our data support that naloxone can effectively downregulate ocular *TLR4* and to inhibit *TNF-α*, *IL-1β*, and oxidative stress mediators of serum NO. The anti-inflammatory and neuroprotective effects are likely through the reduction of microglia activation and accumulation. Naloxone may be considered an alternative therapy to target activated microglia in AMD.

## References

- Iijima I, Minamikawa J, Jacobson AE, Brossi A, Rice KC. Studies in the (+)-morphinan series, 5: synthesis and biological properties of (+)-naloxone. *J Med Chem.* 1978;21:398–400.
- Marcoli M, Ricevuti G, Mazzone A, Pasotti D, Lecchini S, Frigo GM. A stereoselective blockade by naloxone of opioid and non-opioid-induced granulocyte activation. *Int J Immunopharmacol.* 1989; 11:57–61.
- Zhang J, Qian H, Zhao P, Hong SS, Xia Y. Rapid hypoxia preconditioning protects cortical neurons from glutamate toxicity through delta-opioid receptor. *Stroke.* 2006;37:1094–1099.
- Kong LY, McMillian MK, Hudson PM, Jin L, Hong JS. Inhibition of lipopolysaccharide-induced nitric oxide and cytokine production by ultralow concentrations of dynorphins in mixed glia cultures. *J Pharmacol Exp Ther.* 1997;280:61–66.
- Lu X, Bing G, Hagg T. Naloxone prevents microglia-induced degeneration of dopaminergic substantia nigra neurons in adult rats. *Neuroscience.* 2000;97:285–291.
- Liu B, Du L, Hong JS. Naloxone protects rat dopaminergic neurons against inflammatory damage through inhibition of microglia activation and superoxide generation. *J Pharmacol Exp Ther.* 2000; 293:607–617.
- Liu B, Hong JS. Role of microglia in inflammation-mediated neurodegenerative diseases: mechanisms and strategies for therapeutic intervention. *J Pharmacol Exp Ther.* 2003;304:1–7.
- Simpkins CO, Ives N, Tate E, Johnson M. Naloxone inhibits superoxide release from human neutrophils. *Life Sci.* 1985;37:1381–1386.
- Kang J, Park EJ, Jou I, Kim JH, Joe EH. Reactive oxygen species mediate A beta(25–35)-induced activation of BV-2 microglia. *Neuroreport.* 2001;12:1449–1452.
- Dick AD. Influence of microglia on retinal progenitor cell turnover and cell replacement. *Eye (Lond).* 2009;23:1939–1945.
- Langmann T. Microglia activation in retinal degeneration. *J Leukoc Biol.* 2007;81:1345–1351.
- Lee JE, Liang KJ, Fariss RN, Wong WT. Ex vivo dynamic imaging of retinal microglia using time-lapse confocal microscopy. *Invest Ophthalmol Vis Sci.* 2008;49:4169–4176.
- Xu H, Chen M, Manivannan A, Lois N, Forrester JV. Age-dependent accumulation of lipofuscin in perivascular and subretinal microglia in experimental mice. *Aging Cell.* 2008;7:58–68.
- Rivest S. Regulation of innate immune responses in the brain. *Nat Rev Immunol.* 2009;9:429–439.
- Block ML, Hong JS. Microglia and inflammation-mediated neurodegeneration: multiple triggers with a common mechanism. *Prog Neurobiol.* 2005;76:77–98.
- Ding X, Patel M, Chan CC. Molecular pathology of age-related macular degeneration. *Prog Retin Eye Res.* 2009;28:1–18.
- Combadiere C, Feumi C, Raoul W, et al. CX3CR1-dependent subretinal microglia cell accumulation is associated with. *J Clin Invest.* 2007;117:2920–2928.
- Thanos S, Mey J, Wild M. Treatment of the adult retina with microglia-suppressing factors retards axotomy-induced neuronal degradation and enhances axonal regeneration in vivo and in vitro. *J Neurosci.* 1993;13:455–466.
- Jeohn GH, Cooper CL, Jang KJ, et al. Go6976 inhibits LPS-induced microglial TNFalpha release by suppressing p38 MAP kinase activation. *Neuroscience.* 2002;114:689–697.
- Ni YQ, Xu GZ, Hu WZ, Shi L, Qin YW, Da CD. Neuroprotective effects of naloxone against light-induced photoreceptor degeneration through inhibiting retinal microglial activation. *Invest Ophthalmol Vis Sci.* 2008;49:2589–2598.
- Gwak MS, Li L, Zuo Z. Morphine preconditioning reduces lipopolysaccharide and interferon-gamma-induced mouse microglial cell injury via delta 1 opioid receptor activation. *Neuroscience.* 2010;167:256–260.
- Zhang P, Lokuta KM, Turner DE, Liu B. Synergistic dopaminergic neurotoxicity of manganese and lipopolysaccharide: differential involvement of microglia and astroglia. *J Neurochem.* 2010;112: 434–443.

23. Tuo J, Bojanowski CM, Zhou M, et al. Murine ccl2/cx3cr1 deficiency results in retinal lesions mimicking human age-related macular degeneration. *Invest Ophthalmol Vis Sci.* 2007;48:3827-3836.
24. Chan CC, Ross RJ, Shen D, et al. Ccl2/Cx3cr1-deficient mice: an animal model for age-related macular degeneration. *Ophthalmic Res.* 2008;40:124-128.
25. Ross RJ, Zhou M, Shen D, et al. Immunological protein expression profile in Ccl2/Cx3cr1 deficient mice with lesions similar to age-related macular degeneration. *Exp Eye Res.* 2008;86:675-683.
26. Tuo J, Ross RJ, Herzlich AA, et al. A high omega-3 fatty acid diet reduces retinal lesions in a murine model of macular degeneration. *Am J Pathol.* 2009;175:799-807.
27. Zhao L, Ma W, Fariss RN, Wong WT. Retinal vascular repair and neovascularization are not dependent on CX3CR1 signaling in a model of ischemic retinopathy. *Exp Eye Res.* 2009;88:1004-1013.
28. Ben-Shabat S, Parish CA, Hashimoto M, Liu J, Nakanishi K, Sparrow JR. Fluorescent pigments of the retinal pigment epithelium and age-related macular degeneration. *Bioorg Med Chem Lett.* 2001;11:1533-1540.
29. Ma W, Zhao L, Fontainhas AM, Fariss RN, Wong WT. Microglia in the mouse retina alter the structure and function of retinal pigmented epithelial cells: a potential cellular interaction relevant to AMD. *PLoS One.* 2009;4:e7945.
30. Ding AH, Nathan CF, Stuehr DJ. Release of reactive nitrogen intermediates and reactive oxygen intermediates from mouse peritoneal macrophages: comparison of activating cytokines and evidence for independent production. *J Immunol.* 1988;141:2407-2412.
31. Bonfiglio V, Bucolo C, Camillieri G, Drago F. Possible involvement of nitric oxide in morphine-induced miosis and reduction of intraocular pressure in rabbits. *Eur J Pharmacol.* 2006;534:227-232.
32. Stagni E, Bucolo C, Motterlini R, Drago F. Morphine-induced ocular hypotension is modulated by nitric oxide and carbon monoxide: role of mu3 receptors. *J Ocul Pharmacol Ther.* 2010;26:31-35.
33. Tansey MG, McCoy MK, Frank-Cannon TC. Neuroinflammatory mechanisms in Parkinson's disease: potential environmental triggers, pathways, and targets for early therapeutic intervention. *Exp Neurol.* 2007;208:1-25.
34. Wax MB, Tezel G, Yang J, et al. Induced autoimmunity to heat shock proteins elicits glaucomatous loss of retinal ganglion cell neurons via activated T-cell-derived fas-ligand. *J Neurosci.* 2008;28:12085-12096.
35. Perry VH, Nicoll JA, Holmes C. Microglia in neurodegenerative disease. *Nat Rev Neurol.* 2010;6:193-201.
36. Sasahara M, Otani A, Oishi A, et al. Activation of bone marrow-derived microglia promotes photoreceptor survival in inherited retinal degeneration. *Am J Pathol.* 2008;172:1693-1703.
37. Chen L, Wu W, Dentchev T, et al. Light damage induced changes in mouse retinal gene expression. *Exp Eye Res.* 2004;79:239-247.
38. Santos AM, Martin-Oliva D, Ferrer-Martin RM, et al. Microglial response to light-induced photoreceptor degeneration in the mouse retina. *J Comp Neurol.* 2010;518:477-492.
39. Naskar R, Wissing M, Thanos S. Detection of early neuron degeneration and accompanying microglial responses in the retina of a rat model of glaucoma. *Invest Ophthalmol Vis Sci.* 2002;43:2962-2968.
40. Ahmed F, Brown KM, Stephan DA, Morrison JC, Johnson EC, Tomarev SI. Microarray analysis of changes in mRNA levels in the rat retina after experimental elevation of intraocular pressure. *Invest Ophthalmol Vis Sci.* 2004;45:1247-1258.
41. Gehrig A, Langmann T, Horling F, et al. Genome-wide expression profiling of the retinoschisin-deficient retina in early postnatal mouse development. *Invest Ophthalmol Vis Sci.* 2007;48:891-900.
42. Kercher L, Favara C, Striebel JF, LaCasse R, Chesebro B. Prion protein expression differences in microglia and astroglia influence scrapie-induced neurodegeneration in the retina and brain of transgenic mice. *J Virol.* 2007;81:10340-10351.
43. Streit WJ. Microglia and neuroprotection: implications for Alzheimer's disease. *Brain Res Brain Res Rev.* 2005;48:234-239.
44. Wang XJ, Ye M, Zhang YH, Chen SD. CD200-CD200R regulation of microglia activation in the pathogenesis of Parkinson's disease. *J Neuroimmune Pharmacol.* 2007;2:259-264.
45. Gupta N, Brown KE, Milam AH. Activated microglia in human retinitis pigmentosa, late-onset retinal degeneration, and age-related macular degeneration. *Exp Eye Res.* 2003;76:463-471.
46. Chen L, Yang P, Kijlstra A. Distribution, markers, and functions of retinal microglia. *Ocul Immunol Inflamm.* 2002;10:27-39.
47. Sugama S, Takenouchi T, Cho BP, Joh TH, Hashimoto M, Kitani H. Possible roles of microglial cells for neurotoxicity in clinical neurodegenerative diseases and experimental animal models. *Inflamm Allergy Drug Targets.* 2009;8:277-284.
48. Carter DA, Dick AD. Lipopolysaccharide/interferon-gamma and not transforming growth factor beta inhibits retinal microglial migration from retinal explant. *Br J Ophthalmol.* 2003;87:481-487.
49. Shi X, Semkova I, Muther PS, Dell S, Kociok N, Joussen AM. Inhibition of TNF-alpha reduces laser-induced choroidal neovascularization. *Exp Eye Res.* 2006;83:1325-1334.
50. Zheng H, Zhu W, Zhao H, Wang X, Wang W, Li Z. Kainic acid-activated microglia mediate increased excitability of rat hippocampal neurons in vitro and in vivo: crucial role of interleukin-1beta. *Neuroimmunomodulation.* 2010;17:31-38.
51. Zhang JM, An J. Cytokines, inflammation, and pain. *Int Anesthesiol Clin.* 2007;45:27-37.
52. Lin SL, Tsai RY, Tai YH, et al. Ultra-low dose naloxone upregulates interleukin-10 expression and suppresses neuroinflammation in morphine-tolerant rat spinal cords. *Behav Brain Res.* 2010;207:30-36.
53. Beutler B. TLR4 as the mammalian endotoxin sensor. *Curr Top Microbiol Immunol.* 2002;270:109-120.
54. Akira S, Takeda K. Toll-like receptor signalling. *Nat Rev Immunol.* 2004;4:499-511.
55. Lehnardt S, Massillon L, Follett P, et al. Activation of innate immunity in the CNS triggers neurodegeneration through a Toll-like receptor 4-dependent pathway. *Proc Natl Acad Sci U S A.* 2003;100:8514-8519.